Ecotoxicology and Environmental Safety 278 (2024) 116440

Contents lists available at ScienceDirect

Ecotoxicology and Environmental Safety

journal homepage: www.elsevier.com/locate/ecoenv

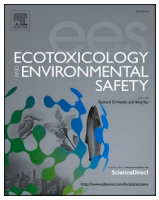

Simulation and parameter determination of the net sorption of phenanthrene by sediment particles

Donglin Yu [a,b], Xinyu Guo [c], Aobo Wang [d], Zhaosen Wu [a,b], Jie Shi [a,b,*]

[a] Key Laboratory of Marine Environment and Ecology, Ocean University of China, Ministry of Education, 238 Songling Road, Qingdao 266100, China
[b] Laboratory for Marine Ecology and Environmental Sciences, Qingdao National Laboratory for Marine Science and Technology, Qingdao 266237, China
[c] Center for Marine Environmental Studies, Ehime University2-5 Bunkyo-cho, Matsuyama 790-8577,Japan
[d] School of Hydraulic Engineering, Ludong University, Yantai, Shandong 264025, China

ARTICLE INFO

Edited by Dr Yong Liang

Keywords:
Polycyclic aromatic hydrocarbons
Sorption-desorption model
Particles
Temperature
Organic carbon content

ABSTRACT

The distribution of polycyclic aromatic hydrocarbons (PAHs) in the ocean is affected by the sorption-desorption process of sediment particles. This process is determined by the concentration of PAHs in seawater, water temperature, and organic matter content of sediment particles. Quantitative relationships between the net sorption rates (=the difference of sorption and desorption rates) and these factors have not been established yet and used in PAH transport models. In this study, phenanthrene was chosen as the representative of PAHs. Three groups of experimental data were collected to address the dependence of the net sorption processes on the initial concentration, water temperature, and organic carbon content representing organic matter content. One-site and two-compartment mass-transfer models were tested to represent the experimental data using various parameters. The results showed that the two-compartment mass-transfer model performed better than the one-site mass-transfer model. The parameters of the two-compartment mass-transfer model include the sorption rate coefficients $k_a^f$and k_a^s (L g^{-1} min^{-1}), and the desorption rate coefficients k_d^f and k_d^s (min^{-1}). The parameters at different temperatures and organic carbon contents were obtained by numerical simulations. Linear relationships were obtained between the parameters and water temperature, as well as organic carbon content. k_a^f, k_a^s and k_d^f decreased linearly, while k_d^s increased linearly with temperature. k_a^f, k_a^s and k_d^f increased linearly, while k_d^s decreased linearly with organic carbon content. The r^2 values between the simulation results based on the relationships and the experimental results reached 0.96–0.99, which supports the application of the model to simulate sorption-desorption processes at different water temperatures and organic carbon contents in a realistic ocean.

1. Introduction

Polycyclic aromatic hydrocarbons (PAHs) are biotoxic and exert carcinogenic, teratogenic, and mutagenic effects on organisms (Chen and Liao, 2006; Hao et al., 2016; Goswami et al., 2018; Alaekwe and Abba, 2022). PAHs are semivolatile and difficult to degrade in the natural environment (Goswami et al., 2017; 2019). They persist in the environment and migrate over long distances (Jones and Voogt, 1999; Wang et al., 2011; Xu et al., 2022). Thus, PAHs are widespread and potentially harmful to the environment. The United States Environmental Protection Agency listed 16 types of PAHs as priority pollutants (USEPA, 1992; IARC, 2007; Zheng and Li, 2017).

The ocean is regarded as a sink of pollutants (Lara-Martin et al., 2020; Wang et al., 2020), and PAHs also exist in it. Concentrations of PAHs in the ocean have been previously reported (Al-Farawati et al., 2009; Zhang et al., 2013; El-Naggar et al., 2021; Shi et al., 2022). PAHs exist not only in aqueous phase (seawater) but also in solid phase (suspended sediment particles) (Neroda et al., 2020; Sakellari et al., 2021; Sun et al., 2021; Wang et al., 2022). PAHs can migrate between aqueous and solid phases through the sorption-desorption process. PAHs in the particles can be transported from the sea surface to the sea bottom by the sinking of particles. Consequently, the sediments are enriched in PAHs (Hu et al., 2010, 2011; Zafarani et al., 2022).

PAHs inside the sediment can return to the water column through the

* Corresponding author at: Key Laboratory of Marine Environment and Ecology, Ocean University of China, Ministry of Education, 238 Songling Road, Qingdao 266100, China.
E-mail address: shijie@ouc.edu.cn (J. Shi).

https://doi.org/10.1016/j.ecoenv.2024.116440
Received 25 January 2024; Received in revised form 16 April 2024; Accepted 3 May 2024
Available online 10 May 2024

resuspension of particles and the diffusion of interstitial water. PAHs in the particles can be released back into seawater through sorption-desorption. The sorption-desorption processes occur in both the water column and the sediment, and their difference results in net sorption amount, which play an important role in the distribution of PAHs in the ocean. Therefore, it is necessary to quantify the net sorption of PAHs between seawater and sediment particles.

Previous studies have used different types of sorption kinetic models to explore the net sorption process, such as first-, second-, pseudo-first- and pseudo-second-order models, to fit data from laboratory experiments (Ho and Mckay, 1999; Oh et al., 2013; Wu et al., 2009; Yang and Zheng, 2010). In the laboratory experiment, the net sorption rate was determined by the amount of sorbed pollutant in the particles until the equilibrium state was reached, which cannot be directly observed in realistic oceans. Therefore, these models are not suitable for simulating the net sorption processes in realistic oceans. Nzengung et al. (1997) applied a one-site mass-transfer model to calculate the net sorption rate of naphthalene using organic clay. This model was later used to describe the net sorption of hydrophobic organic pollutants (Oh et al., 2011, 2013). Ding et al. (2008) divided the net sorption into fast and slow processes, established a two-compartment mass-transfer model, and achieved good agreement in simulating the net sorption process of hexachlorobenzene. In the one-site mass-transfer model and two-compartment mass-transfer model, the net sorption rate can be calculated as the difference between the concentrations of pollutants in the aqueous and solid phases, which can be observed in realistic oceans. Thus, these two models are suitable for simulating the net sorption processes in realistic oceans. However, these models have not been used to simulate the transport of pollutants in the ocean (Wang et al., 2019). The addition of a sorption-desorption module to the pollutant transport model is preferred. Before this, we need to quantify the impact of the factors on the sorption-desorption process.

In laboratory experiments, certain conditions such as the initial concentration of the pollutant or water temperature can be fixed. By changing only one condition, the parameters related to this condition in the model can be determined by fitting the model results to the experimental data. Different experimental conditions were expected to affect the net sorption results. Experiments have shown that net sorption processes vary with the initial concentration of pollutant (Shi et al., 2015), water temperature (Zhu et al., 2006), and organic carbon content (representing organic matter content) of the sediment particles (Wang et al., 2008). Because these conditions are always changing in the realistic ocean, it is necessary to establish quantitative relationships between the parameters of the sorption-desorption models and these conditions, including the initial concentration of PAHs, water temperature, and organic carbon content. This supports the embedding of the net sorption model into pollutant transport models in the ocean.

This study aimed to accurately simulate the net sorption processes of phenanthrene, a representative PAH, in marine environments. To achieve this goal, tuning the parameters to make the model results approach to the experimental data, and then the optimal parameters of the one-site and two-compartment mass-transfer models were obtained. Quantitative relationships were then established between the model parameters and the initial concentration of phenanthrene, water temperature, as well as organic carbon content of the sediment particles. The contributions of fast and slow processes in the two-compartment mass-transfer model were analyzed. The differences between the net sorption models of sediment particles and phytoplankton were discussed. Finally, we explored the temperature dependence of the two-compartment mass-transfer model in a realistic coastal ocean simulation. This study lays the foundation for embedding the sorption-desorption model into pollutant transport models.

2. Methods

2.1. Model descriptions

2.1.1. One-site mass-transfer model

In the one-site mass-transfer model (Nzengung et al., 1997), the net sorption rate was set as a first-order function of the concentration difference between the aqueous and solid phases. The net sorption rate is expressed as follows:

$$\frac{dC_p}{dt} = k_s^a \bullet (K_p \bullet C_d - C_p) \tag{1}$$

$$K_p = \frac{C_{pe}}{C_{de}} \tag{2}$$

where C_p (mg g^{-1}) and C_d (mg L^{-1}) are the concentrations of the solid and aqueous phases, respectively. In Eq. (1), C_d is converted to the corresponding concentration of the solid phase in the theoretical sorption equilibrium state by multiplying with the partition equilibrium coefficient (K_p, L g^{-1}). C_{pe} (mg g^{-1}) and C_{de} (mg L^{-1}) are the concentrations in the solid and aqueous phases, respectively, when sorption-desorption reaches equilibrium. k_s^a (min^{-1}) is the mass transfer coefficient, which represents the linear relationship between the net sorption rate and concentration difference.

2.1.2. Two-compartment mass-transfer model

In the two-compartment mass-transfer model, the net sorption process is divided into fast and slow processes (Ding et al., 2008). Consequently, the pollutant concentration in the solid phase (C_p) also have two components: the concentrations of fast (C_p^f, mg g^{-1}) and slow processes (C_p^s, mg g^{-1}). The net sorption rates of the fast and slow processes can be expressed as

$$\frac{dC_p^f}{dt} = k_a^f \bullet C_d - k_d^f \bullet C_p^f \tag{3}$$

$$\frac{dC_p^s}{dt} = k_a^s \bullet C_d - k_d^s \bullet C_p^s \tag{4}$$

where $k_a^f$and k_a^s (L g^{-1} min^{-1}) are the sorption rate coefficients, and $k_d^f$and k_d^s (min^{-1}) are the desorption rate coefficients, $k_a^f \bullet C_d$and $k_a^s \bullet C_d$ are sorption rates for the fast and slow processes, and $k_d^f \bullet C_p^f$and $k_d^s \bullet C_p^s$ are desorption rates for the fast and slow processes. The net sorption rate is the sum of the two processes and can be expressed as

$$\frac{dC_p}{dt} = \frac{dC_p^f}{dt} + \frac{dC_p^s}{dt} = (k_a^f \bullet C_d - k_d^f \bullet C_p^f) + (k_a^s \bullet C_d - k_d^s \bullet C_p^s) \tag{5}$$

2.2. Experimental data

The experimental data to test the simulation results were obtained from the measured net sorption processes of phenanthrene between sediment particles and seawater reported by the other studies (Yang and Zheng, 2010; Zheng, 2010; Xu and Huang, 2011).

Different phenanthrene concentrations in seawater will result in different net sorption capacity. The experimental data of Yang and Zheng (2010) were used to conduct numerical simulations to explore the responses of model parameters to different phenanthrene concentrations. The experimental data were the phenanthrene concentrations in sediment particles measured at 11 time points through the net sorption using three different initial concentrations of phenanthrene in seawater. The data of each time point was obtained through 3 measurements.

In addition, numerical simulations were carried out using the experimental data of net sorption kinetics given by Zheng (2010) to discuss the parameters of the sorption-desorption models at different

temperatures. This experimental data were the phenanthrene concentrations in sediment particles measured at 11 time points through the net sorption at three different water temperatures. The data of each time point was obtained through 3 measurements.

Similarly, the experimental data of net sorption kinetics given by Xu and Huang (2011) showed the concentrations of phenanthrene in water at 9 time points through the net sorption process at four different organic carbon contents of sediment particles. The results were obtained by conducting 2 parallel experiments. In this study, based on the mass conservation of total phenanthrene in the water and sediment particles, the concentration of phenanthrene in the sediment particles at each time point was obtained. The relationship between parameters of the two models given in Section 2.1 and organic carbon content was determined by numerical simulations.

The above experimental data were arranged into three groups, and used to determine model parameters under different phenanthrene concentrations in seawater (Group I), water temperatures (Group II), and organic carbon contents of the sediment particles (Group III). It must be noted that these experimental data were the results of previous studies and the specific experimental methods are given in the corresponding papers (Yang and Zheng, 2010; Zheng, 2010; Xu and Huang, 2011). A brief description on each group is provided in Text S1 in the Supplementary Materials.

2.3. Numerical simulations

In MATLAB (R2022b), the numerical solution of Eq. (1) and (5) were approached to each group of experimental data by tuning parameters, and the optimal parameters of the models were determined from the solution that has the minimum difference from the experiment data. Based on these determined optimal parameters, the dependences of the parameters in Eq. (1) and (5) on the initial phenanthrene concentration in seawater, water temperature, and organic carbon content of the sediment particles were examined. After knowing the dependences, the model simulation can be carried out for any initial phenanthrene concentration in seawater, any water temperature, and any organic carbon content of the sediment particles, which exist in the realistic ocean. The determination coefficient (r^2) and sums of squares of error (*SSE*) between the model results and the experimental data were calculated to evaluate the performance of the simulations.

3. Results

3.1. Influence of the initial concentration in seawater on net sorption values

The net sorption experimental data for Group I were obtained for three different initial pollutant concentrations. The parameters determination and simulation results of the one-site and two-compartment mass-transfer models in Group I are given in Text S2 of the Supplementary Materials. The simulation results showed that the two-compartment mass-transfer model performed better than the one-site mass-transfer model.

In the one-site mass-transfer model, k_s^a represents the exchange rate of phenanthrene between seawater and sediment particles, and K_p represents the transporting trend of phenanthrene from seawater to sediment particles. k_s^a and K_p did not differ significantly among the three experiments (Table S1). When one set of parameters was used to simulate all three experiments, the value of r^2 reached 0.9710, indicating that a fixed set of parameters can accurately reproduce the three experiments. In other words, the initial concentration of phenanthrene in seawater had little impact on the k_s^a and K_p values (Fig. 1). By tuning the parameters, the optimal k_s^a and K_p were determined to be 0.342 min^{-1} and 0.1197 L g^{-1}, which achieved the highest r^2 of 0.9738 (Table S2).

In the two-compartment mass-transfer model, k_a^f and k_a^s represent the migration rates of phenanthrene from seawater to sediment particles and k_d^f and k_d^s represent the migration rates from sediment particles to seawater. k_a^f and k_d^f determine the net sorption rate of the fast process, and k_a^s and k_d^s determine the net sorption rate of the slow process. k_a^f, k_a^s, k_d^f, and k_d^s showed little change at the three different initial concentrations (Table S1). Thus, similar to the one-site mass-transfer model, a fixed set of parameters was used in all three experiments (Fig. 1). k_a^f, k_a^s, k_d^f, and k_d^s were tuned to obtain a set of optimal values to reduce the bias between the model results and the experimental data, which were 0.0395 L g^{-1} min^{-1}, 0.00391 L g^{-1} min^{-1}, 0.482 min^{-1}, and 0.0815 min^{-1}, respectively (Table S2), obtaining an r^2 of up to 0.9931.

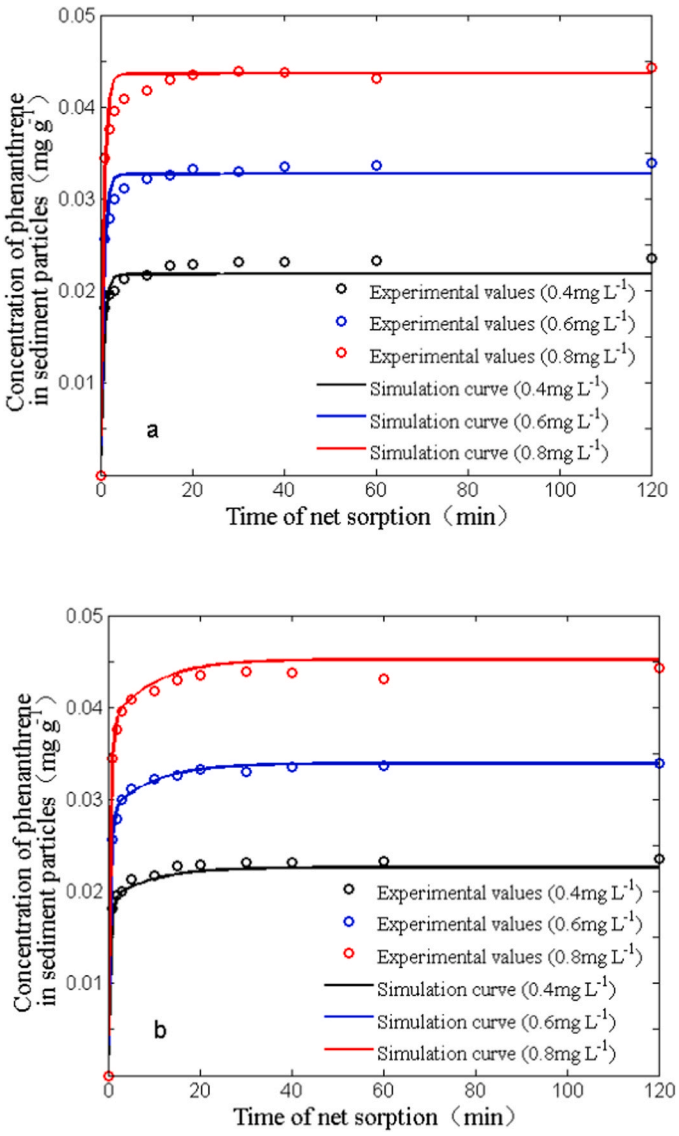

Fig. 1. Simulation curves of the two sorption kinetics models for phenanthrene at different initial concentrations with the same set of parameters. a: One-site mass-transfer model. b: Two-compartment mass-transfer model.

The results show that each model can reproduce the experimental data using a set of parameters for different initial concentrations. Therefore, it is feasible to use a set of parameters for ocean simulations with variable PAH concentrations.

3.2. Influence of the water temperature on net sorption values

The experiments in Group II tested the dependence of the net sorp-

tion curves on the water temperature. The parameters determination and simulation results of the two models are provided in Text S3. Based on the parameters determination results of these three experiments (Table S3), quantitative relationships between the parameters in the one-site mass-transfer model and the water temperature were established, which are expressed as follows:

$$k_s^a = 0.0071 \bullet T + 0.1333 \quad (6)$$

$$K_p = -0.0045 \bullet T + 0.2467 \quad (7)$$

where T is the water temperature (℃).

When considering the dependence of the parameters on water temperature in the one-site mass-transfer model (Fig. 2), the r^2 was high, at up to 0.9504, and *SSE* was 9.24×10^{-5} for the three water temperature experiments (Table S4). However, when using fixed values of the parameters from one experiment under a given water temperature, the maximum r^2 was only 0.8606, indicating a weaker accuracy of the simulations.

In the two-compartment mass-transfer model, the linear relationships between the four parameters and the water temperature were established and expressed as follows:

$$k_a^f = -0.000445 \bullet T + 0.0504 \quad (8)$$

$$k_a^s = -0.000181 \bullet T + 0.0085 \quad (9)$$

$$k_d^f = -0.0008 \bullet T + 0.4943 \quad (10)$$

$$k_d^s = 0.0022 \bullet T + 0.0333 \quad (11)$$

when the linear relationships between the parameters and the water temperature in Eqs. (8)–(11) were considered, the mean r^2 reached up to 0.9963, with an *SSE* of 6.06×10^{-6} (Table S4), which indicated a better performance of the model (Fig. 2).

The accuracy of the simulations was improved by considering the dependence of the model parameters on water temperature. Moreover, it has become more reasonable and feasible to apply these models to realistic oceans with spatially and temporally changes in the water temperature.

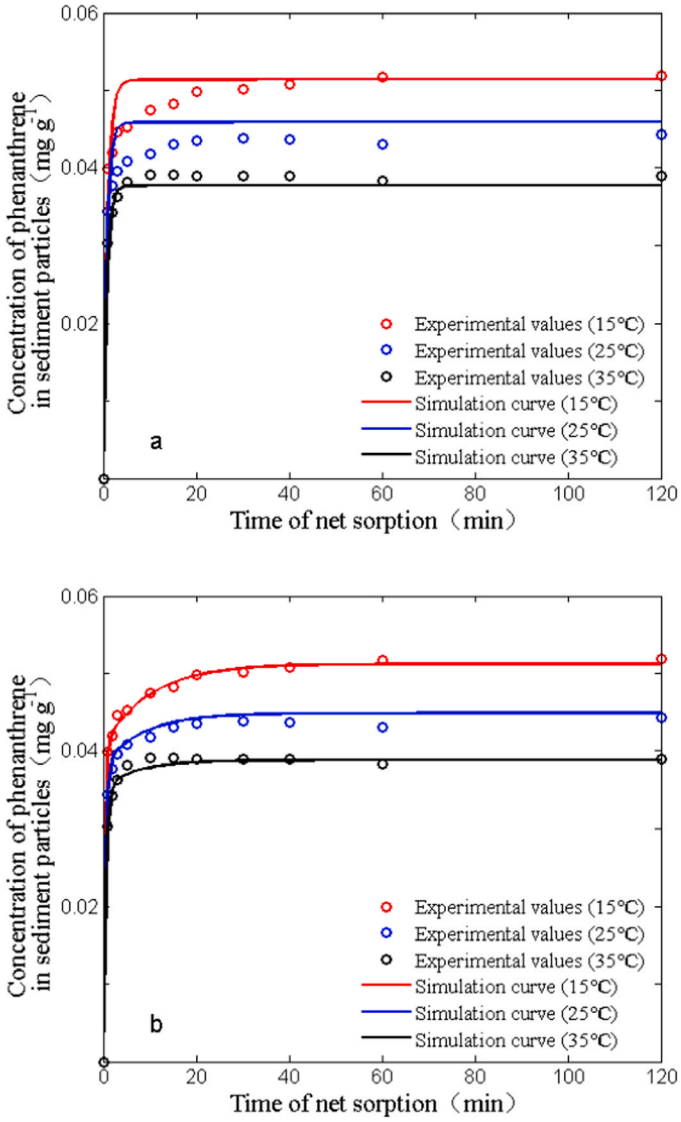

Fig. 2. Simulation curves of the two sorption kinetics models considering the dependence of the parameters on the water temperature. a: One-site mass-transfer model. b: Two-compartment mass-transfer model.

3.3. Influence of the organic carbon content of sediment particles on net sorption values

The experiments in Group III showed the net sorption curves of the sediment particles with four different organic carbon contents. The parameters determination and simulation results of the two models are provided in Text S4 of the Supplementary Materials. The parameters were assumed to be linear functions of the organic carbon content. In the one-site mass-transfer model, the linear relationships between k_s^a and K_p and the organic carbon content are expressed as follows:

$$k_s^a = -0.2579 \bullet f_{oc} + 0.0148 \quad (12)$$

$$K_p = 29.0077 \bullet f_{oc} - 0.0527 \quad (13)$$

where f_{oc} is the organic carbon content (%).

When using Eqs. (12) and (13) in the one-site mass-transfer model (Fig. 3), the mean values of r^2 and *SSE* were 0.9411 and 1.98×10^{-4}, respectively (Table S6). When fixed values of k_s^a and K_p, the optimal r^2 was only 0.7139, indicating the importance of considering the dependence of the model parameters on the organic carbon content.

The linear relationships between the parameters in the two-compartment mass-transfer model and the organic carbon content were obtained as follows:

$$k_a^f = 0.3321 \bullet f_{oc} + 0.00036108 \quad (14)$$

$$k_a^s = 0.0495 \bullet f_{oc} - 0.00017075 \quad (15)$$

$$k_d^f = 0.2554 \bullet f_{oc} + 0.0271 \quad (16)$$

$$k_d^s = -0.0258 \bullet f_{oc} + 0.0033 \quad (17)$$

When considering the dependence of the parameters on the organic carbon content of the sediment particles (Fig. 3), the results showed that r^2 was up to 0.9612 and *SSE* was 1.35×10^{-4} (Table S6). However, if the dependences of the parameters on organic carbon content is ignored, the optimal r^2 was only 0.7600. The results showed that the simulation accuracy significantly improved by changing the model parameters for different organic carbon contents.

4. Discussion

4.1. Two processes of the two-compartment mass-transfer model

As indicated by the higher values of determination coefficient with the experimental data in the simulations, the two-compartment mass-transfer model performed much better than the one-site mass-transfer

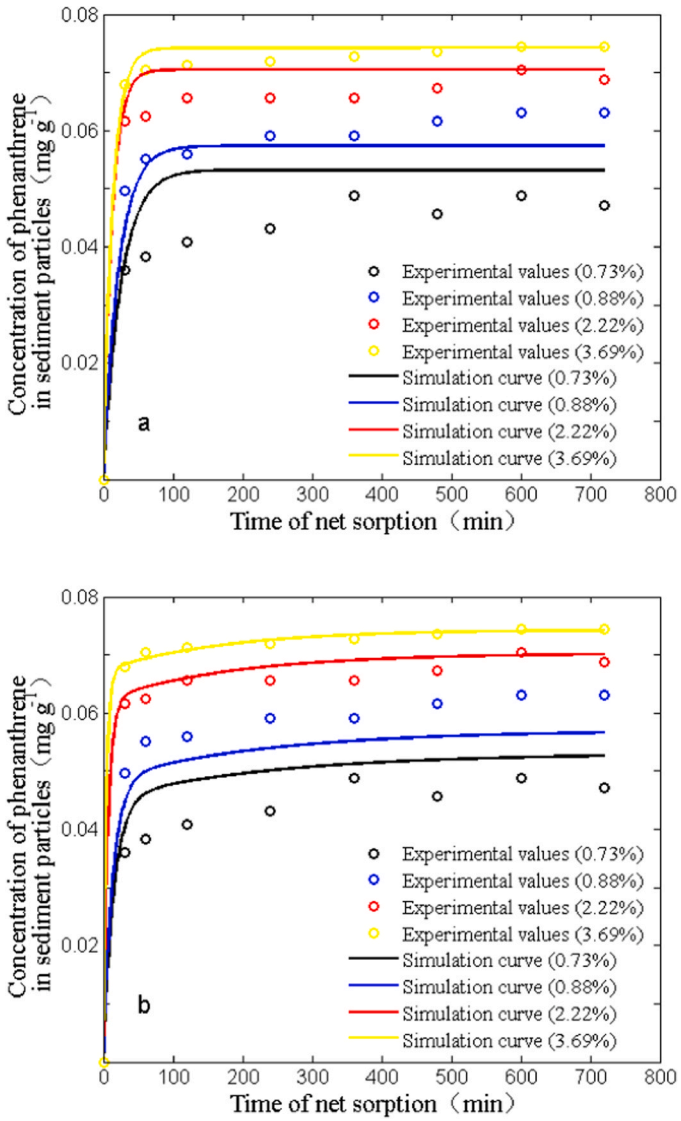

Fig. 3. Simulation curves of the two sorption kinetics models considering the dependence of the parameters on the organic carbon contents. a: One-site mass-transfer model. b: Two-compartment mass-transfer model.

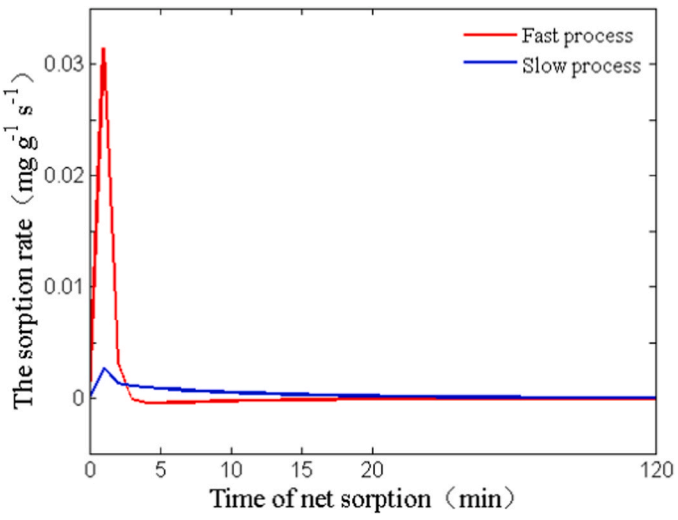

Fig. 4. Variations of the sorption rates of fast and slow processes in the two-compartment mass-transfer model.

model in all experiments for the three groups. To evaluate the contributions of fast and slow processes in the two-compartment mass-transfer model, a new simulation was carried out under the initial concentration of 0.8 mg L^{-1}, organic carbon content of sediment of 0.75 %, and water temperature of 25 ℃.

The net sorption rates of the fast and slow processes were calculated and compared (Fig. 4). The net sorption rate of the fast process increased sharply at the beginning and reached its peak value of 0.0314 mg g^{-1} s^{-1} at 1 min. Subsequently, it rapidly decreased to below zero at 2.5 min. It then gradually increased to zero and remained almost constant until the end of the experiment. The net sorption rate of the slow process was significantly lower than that of the fast process. It also increased at the beginning and peaked at 0.0027 mg g^{-1} s^{-1} at 1 min, which was only about 10 % of that of the fast process. It then gradually decreased to approximately zero at 120 min but had no negative value during the entire experiment.

The fast and slow net sorption processes were attributed to the structures of the sediment particles. The composition of sediment particles includes inorganic surfaces, amorphous and condensed organic matter (Walter et al., 1996), which plays a dominant role in the net sorption (Zhang et al., 2016). The surface of sediment particles usually consists of the amorphous organic matter (Xing and Pignatello, 1997; Fan et al., 2010), the unconsolidated structure of which guarantees the fast net sorption of phenanthrene in seawater. The concentration of the phenanthrene at the surface of the amorphous organic matter increased rapidly, whereas that in seawater decreased. When the concentration in the solid phase exceeded that in seawater, phenanthrene desorbed from the sediment particles into the seawater, which induced a negative net sorption rate of the fast process. Finally, the fast net sorption reached its equilibrium state when the difference in concentrations disappeared. Therefore, the sorption rate remained zero.

The inner parts of the sediment particles are occupied by condensed organic matter, which has no opportunity to directly reach the phenanthrene (Fan et al., 2010; Werner et al., 2012). Phenanthrene is sorbed only when it diffuses through the pores in sediment particles and reaches the inner part. Therefore, the net sorption rate of the slow process was comparably low but lasted a longer time.

The two-compartment mass-transfer model expresses the two simultaneous net sorption processes caused by different components of sediment particles. Therefore, this model achieved better agreement with the results of experiment. And the results of the two-compartment mass-transfer model are used in the following discussion.

4.2. Comparisons of the net sorption processes of sediment particles and phytoplankton

PAHs have been detected not only in sediment particles but also in phytoplankton (Tao et al., 2017; Duarte et al., 2021; Castro-Jimenez et al., 2021), indicating that PAHs in the ocean can also be sorbed by phytoplankton (Cerezo et al., 2017). Unlike sediment particles, phytoplankton are living organisms. Therefore, their net sorption process is expected to differ from that of the sediment.

Previous studies have also divided the net sorption processes of phytoplankton into two parts: net sorption of the surface and net sorption of the internal matrix (Dachs et al., 1999). The net sorption rates of pollutants on the surface of phytoplankton are faster than those in the internal matrix (Vento and Dachs, 2002), similar to the fast and slow processes of sediment particles described in the two-compartment mass-transfer model in this study. The structure of the net sorption model for phytoplankton was similar to that of the two-compartment mass-transfer model, which was determined using four parameters: surface sorption rate coefficient k_{ad} (L g^{-1}OC min^{-1}), desorption rate coefficient k_{des} (L g^{-1}OC min^{-1}), matrix sorption rate coefficient k_{it} (min^{-1}), and desorption rate coefficient k_d' (min^{-1}) (Dachs et al., 1999).

For phenanthrene, the values of k_{ad}, k_{des}, k_u, and $k_d^{'}$ were 2.80 L g^{-1}OC min^{-1}, 0.117 min^{-1}, 0.00440 L g^{-1}OC min^{-1}, and 0.000285 min^{-1}, respectively (Table 1). In the net sorption model of phytoplankton, the organic matter in phytoplankton is thought to be fully responsible for the net sorption of phenanthrene. If the organic matter in sediment particles is thought to be fully responsible for the net sorption of phenanthrene, the governing equation of the two-compartment mass-transfer model is as follow:

$$\frac{dC_p^{'}}{dt} = \frac{dC_p^{f^{'}}}{dt} + \frac{dC_p^{s^{'}}}{dt} = (k_a^{f^{'}} \bullet C_d - k_d^{f^{'}} \bullet C_p^{f^{'}}) + (k_a^{s^{'}} \bullet C_d - k_d^{s^{'}} \bullet C_p^{s^{'}}) \quad (18)$$

where $C_p^{'}$ is phenanthrene concentration in organic matter (mg g^{-1} OC). $k_a^{f^{'}}$ and $k_a^{s^{'}}$ (L g^{-1}OC min^{-1}) are the sorption rate coefficients of organic matter in the sediment particles of the fast and slow processes, respectively, and $k_d^{f^{'}}$ and $k_d^{s^{'}}$ (min^{-1}) are the desorption rate coefficients of organic matter in the sediment particles of the fast and slow processes, respectively. The relationship between C_p and $C_p^{'}$ is as follows:

$$C_p^{'} = \frac{C_p}{f_{oc}} \quad (19)$$

Therefore, Eq. (18) can be expressed as

$$\frac{dC_p}{dt} = \frac{dC_p^f}{dt} + \frac{dC_p^s}{dt} = (f_{oc} \bullet k_a^{f^{'}} \bullet C_d - k_d^{f^{'}} \bullet C_p^f) + (f_{oc} \bullet k_a^{s^{'}} \bullet C_d - k_d^{s^{'}} \bullet C_p^s) \quad (20)$$

Comparing with Eq. (5), k_a^f, k_a^s, k_d^f, and k_d^s can be expressed as

$$k_a^f = f_{oc} \bullet k_a^{f^{'}} \quad (21)$$

$$k_a^s = f_{oc} \bullet k_a^{s^{'}} \quad (22)$$

$$k_d^f = k_d^{f^{'}} \quad (23)$$

$$k_d^s = k_d^{s^{'}} \quad (24)$$

where $k_a^{f^{'}}$, $k_a^{s^{'}}$, $k_d^{f^{'}}$, and $k_d^{s^{'}}$ are the parameters similar to those in the net sorption model of phytoplankton. The relationship between the parameters of the two-compartment mass-transfer model and the organic carbon content of sediment particles in Section 3.3 (Eqs. (14)–(17)) indicate that k_a^f and k_a^s are dominated by terms related to f_{oc}, while k_d^f and k_d^s are dominated by terms unrelated to f_{oc}, which is consistent with Eqs. (21)–(24). Therefore, it is reasonable to assume that organic matter in sediment particles is fully responsible for the net sorption of phenanthrene.

The net sorption processes of phenanthrene in the sediment particles and phytoplankton were evaluated by comparing the parameters of the two net sorption models. The parameters in the two-compartment mass-transfer model derived in Group I were used as examples. k_a^f, k_a^s, k_d^f, and k_d^s were converted to $k_a^{f^{'}}$, $k_a^{s^{'}}$, $k_d^{f^{'}}$, and $k_d^{s^{'}}$ by Eqs. (21)–(24) and were compared with those of the net phytoplankton sorption model (Table 1).

Table 1
Parameters of the net sorption models of phenanthrene by sediment particles and phytoplankton.

Parameters of the net sorption	
By sediment particles	By phytoplankton (Vento and Dachs, 2002)
$k_a^{f^{'}}$(L g^{-1}OC min^{-1}) = 5.27	k_{ad}(L g^{-1}OC min^{-1}) = 2.80
$k_a^{s^{'}}$(L g^{-1}OC min^{-1}) = 0.521	k_u(L g^{-1}OC min^{-1}) = 0.00440
$k_d^{f^{'}}$(min^{-1}) = 0.482	k_{des}(min^{-1}) = 0.117
$k_d^{s^{'}}$(min^{-1}) = 0.0815	$k_d^{'}$(min^{-1}) = 0.000285

$k_a^{f^{'}}$ and k_{ad} were of the same order of magnitude, as were the $k_d^{f^{'}}$ and k_{des}. It suggested that the net sorption rates of phenanthrene by sediment particles and by phytoplankton in the fast process were comparable. $k_a^{f^{'}}/k_d^{f^{'}}$ and k_{ad}/k_{des} represent the accumulation capacity of phenanthrene in sediment particles and phytoplankton in the fast process, respectively. $k_a^{f^{'}}/k_d^{f^{'}}$ was 10.93 L g^{-1}, which was only half of the value of k_{ad}/k_{des} (23.93 L g^{-1}), indicating the accumulation capacity of phytoplankton was stronger than that of sediment particles in the fast process.

During the slow process, $k_a^{s^{'}}$ and $k_d^{s^{'}}$ were two orders of magnitude larger than k_u and $k_d^{'}$, suggesting that the exchange rates of phenanthrene between the seawater and sediment particles were much faster than those between the seawater and phytoplankton. The value of $k_a^{s^{'}}/k_d^{s^{'}}$ was 6.39 L g^{-1}, which was much smaller than $k_u/k_d^{'}$ (15.44 L g^{-1}), suggesting that the accumulation capacity of phytoplankton was also stronger than that of sediment particles in the slow process.

In addition, the net sorption kinetics models of different types of pollutants are also different. For inorganic pollutants, the net sorption processes of inorganic phosphorus (Li et al., 2018) and divalent mercury (Tuzen et al., 2009; Sahu et al., 2022) are often simulated by pseudo-first-order and pseudo-second-order kinetic models. The pseudo-second-order kinetic model is more suitable for the net sorption of hexavalent chromium onto activated carbon than the pseudo-first-order kinetic model (Malwade et al., 2016). The above two models describe the net sorption rate as a first- and second- order function of the difference between the final equilibrium sorption amount in the experiment and the current sorption amount in the experiment, respectively. These two models can reproduce the corresponding experimental data. Since the initial concentration of pollutants in medium of each experiment is determined, the final equilibrium sorption amount is unique. In the actual environment, the concentration of pollutants in the medium is changing, and the net sorption is difficult to reach the equilibrium, and the final equilibrium sorption amount cannot be observed. Therefore, it is difficult to apply these models to simulate the net sorption process in a realistic ocean environment. The description of the net sorption rate by the models in this study took into account the change of pollutant concentration in the environmental medium such as the concentration of phenanthrene in seawater.

4.3. Influence of the water temperature on simulation of net sorption process in the Bohai Sea

In Section 3.2, linear relationships between the parameters in the model and water temperatures were established, which made it practical to apply the net sorption model in a realistic ocean with changing temperatures. The Bohai Sea is a semi-enclosed sea located in northeastern China (Fig. S4, 37–41°N, 117–122°E) with an average depth of 18 m. The water temperature of the Bohai Sea exhibited apparent seasonal variations (Fig. S5) (Ding et al., 2021). The influences of the water temperature on the net sorption process of phenanthrene were studied by comparing the simulation under the seasonal variations of temperature and the result of the net sorption at an average temperature of 15℃.

The observed concentration of phenanthrene in surface sediment was 34.4 ng g^{-1} in the Bohai Sea (Hu et al., 2011). At the average bottom water temperature of 15℃, the concentration of phenanthrene in the seawater was calculated to be 193.7 ng L^{-1} when reaching the equilibrium state (the blue horizontal line in Fig. 5). The organic carbon content was set to 0.75%. If the parameters were fixed to the values at 15℃ in the two-compartment mass-transfer model, the concentration of phenanthrene in the sediment particles remained 34.4 ng g^{-1} all year round, although considering the seasonal variations of the water temperature.

Considering the dependence of the model parameters on water temperature, the two-compartment mass-transfer model was used to

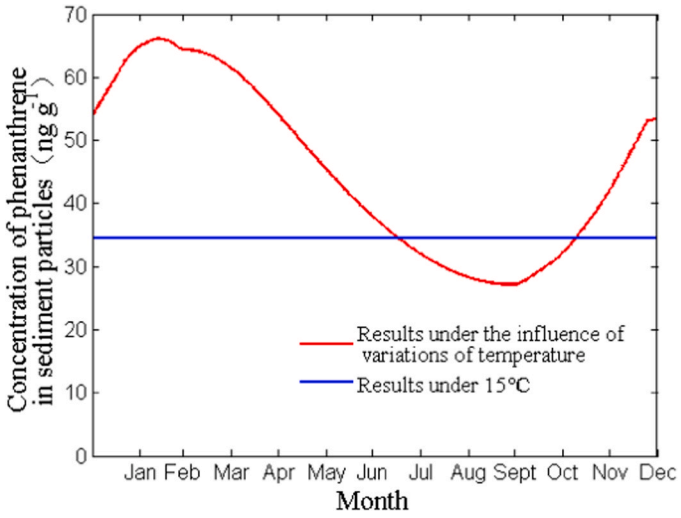

Fig. 5. Simulated seasonal variations of the phenanthrene concentrations in the sediment particles in the Bohai Sea.

simulate the annual cycle of the phenanthrene concentrations in the sediment particles under seasonal variations in the bottom water temperature. The model was integrated for 3 years, and the results in the third year were used for analysis. The model results (the red horizontal line in Fig. 5) showed that the concentration of phenanthrene in the sediment particles increased to the maximum of 66.1 ng g^{-1} in February (day 43) and then gradually decreased to its minimum value of 27.1 ng g^{-1} in September (day 271). In winter, it gradually increased as the water temperature decreased. Regardless of the dependence of the net sorption-related parameters on water temperature, the maximum underestimation and overestimation reached 48.0% and 26.9%, respectively. The average bias of the concentration was 10.9 ng g^{-1}, accounting for approximately 24.1% of average concentration (45.3 ng g^{-1}).

There are still some limitations in this study. Compared with the laboratory experiment, the pollutants sorbed by sediment particles in the ocean are not only phenanthrene, but also other PAHs and even other persistent organic pollutants (POPs). Due to different spatial scales, the molecular dynamics in the actual ocean are probably different from those in laboratory experiments. In similar oceanographic studies, parametric schemes are also derived from experiments and have been applied with good results, such as simulation of phytoplankton growth and fate of POPs in the ocean (Gao et al., 2020; Wang et al., 2019). With such previous research experience, we believe that this study, which also use the laboratory experimental data to finish the parameterization of sorption-desorption process, really lay a foundation for further research in the simulations in the realistic ocean.

5. Conclusions

Based on the published experimental results on the net sorption of phenanthrene by sediment particles, one-site and two-compartment mass-transfer models were used to simulate the net sorption processes. The two-compartment mass-transfer model performed much better than the one-site mass-transfer model in the simulations. By quantifying the dependence of the model parameters on various factors, the influences of the initial concentration, water temperature, and organic carbon content of the sediment particles on the net sorption of phenanthrene were analyzed. This supports the simulation of the two-compartment mass-transfer model in a realistic ocean with variable factors. The usability of the model was proven by analyzing the mechanism of the two-compartment mass-transfer model, comparing it with the phytoplankton model, and simulating the net sorption process in the ocean at different temperatures.

Further improvements are required in this study. Estimations of the parameters of the two-compartment mass-transfer model largely depended on the three selected laboratory experiments. Thus, additional sorption kinetics experiments must be conducted to verify the accuracy of the parameters in the model.

In future studies, similar methods can be used to determine the sorption-desorption parameters of other PAHs and POPs. In addition, the results of this study make it possible to simulate the distribution and fate of PAHs in both seawater and sediment by embedding a net sorption module into the transport model of PAHs, which improves the accuracy of the simulation. Moreover, the parameters can be adjusted according to the comparison between the simulated results and the observations, and the sorption-desorption parameters suitable for other PAHs and POPs can be determined.

CRediT authorship contribution statement

Xinyu Guo: Writing – review & editing, Supervision, Resources, Methodology, Funding acquisition, Conceptualization. **Donglin Yu:** Writing – review & editing, Writing – original draft, Visualization, Validation, Methodology, Investigation, Data curation. **Aobo Wang:** Visualization, Supervision, Methodology. **Jie Shi:** Writing – review & editing, Supervision, Resources, Methodology, Funding acquisition. **Zhaosen Wu:** Visualization, Methodology.

Declaration of Competing Interest

The authors declare that they have no known competing financial interests or personal relationships that could have appeared to influence the work reported in this paper.

Data Availability

The authors do not have permission to share data.

Acknowledgments

This study was supported by the National Natural Science Foundation of China (NSFC) (41976013). X. Guo was supported by a Grant-in-Aid for Scientific Research (MEXT KAKENHI, grant number: 20KK0239). D. Yu was supported by the Ministry of Education, Culture, Sports, Science and Technology, Japan (MEXT) to a project on JointUsage/Research Center–Leading Academia in Marine and Environment Pollution Research (LaMer).

Appendix A. Supporting information

Supplementary data associated with this article can be found in the online version at doi:10.1016/j.ecoenv.2024.116440.

References

Alaekwe, I.O., Abba, O., 2022. Polycyclic aromatic hydrocarbons in water: a review of the sources, properties, exposure pathways, bionetwork and strategies for remediation. J. Geosci. Environ. Prot. 10 (8), 137–144. https://doi.org/10.4236/gep.2022.108010.

Al-Farawati, R.K., El-Maradny, A., Niaz, G.R., 2009. Fecal sterols and PAHs in sewage polluted marine environment along the eastern red sea coast, south of jeddah, saudi arabia. Indian J. Mar. Sci. 38 (4), 404–410. https://doi.org/10.1093/icesjms/fsp206.

Castro-Jimenez, J., Bnaru, D., Chen, C.T., Jimenez, B., Munoz-Arnanz, J., Deviller, G., et al., 2021. Persistent organic pollutants burden, trophic magnification and risk in a pelagic food web from coastal NW Mediterranean Sea. Environ. Sci. Technol. 55, 9557–9568. https://doi.org/10.1021/acs.est.1c00904.

Cerezo, M.I., Linden, M., Agusti, S., 2017. Flow cytometry detection of planktonic cells with polycyclic aromatic hydrocarbons sorbed to cell surfaces. Mar. Pollut. Bull. 118, 64–70. https://doi.org/10.1016/j.marpolbul.2017.02.006.

Chen, S.C., Liao, C.M., 2006. Health risk assessment on human exposed to environmental polycyclic aromatic hydrocarbons pollution sources. Sci. Total Environ. 366 (1), 112–123. https://doi.org/10.1016/j.scitotenv.2005.08.047.
Dachs, J., Eisenreich, S.J., Baker, J.E., Ko, F., Jeremiason, J.D., 1999. Coupling of phytoplankton uptake and air-water exchange of persistent organic pollutants. Environ. Sci. Technol. 33, 3653–3660. https://doi.org/10.1021/es990168o.
Ding, X.K., Guo, X.Y., Gao, H.W., Gao, J., Shi, J., Yu, X.J., et al., 2021. Seasonal variations of nutrient concentrations and their ratios in the central Bohai Sea. Sci. Total Environ. 799, 1–13. https://doi.org/10.1016/j.scitotenv.2021.149416.
Ding, H., Li, X.G., Xu, S.M., Sun, Y.C., Shao, X.L., 2008. HCB adsorption- desorption behavior in suspended sediment. J. Agro Environ. Sci. 27 (2), 711–715. https://doi.org/10.3321/j.issn:1672-2043.2008.02.056.
Duarte, B., Gameiro, C., Matos, A.R., Figueiredo, A., Silva, M.S., Cordeiro, C., et al., 2021. First screening of biocides, persistent organic pollutants, pharmaceutical and personal care products in antarctic phytoplankton from deception island by FT-ICR-MS. Chemosphere 274, 1–12. https://doi.org/10.1016/j.chemosphere.2021.129860.
El-Naggar, M., Hanafy, S., Younis, A.M., Ghandour, M.A., El-Sayed, A.A.Y., 2021. Seasonal and temporal influence on polycyclic aromatic hydrocarbons in the Red Sea coastal water, Egypt. Sustainability 13 (21), 11906. https://doi.org/10.3390/su132111906.
Fan, S.L., Tian, D.Y., Han, X.X., 2010. Adsorption and desorption behavior of phenanthrene and pyrene on sediments of Huai River, Yellow River and Wei River. Environ. Pollut. Cont. 32 (5), 34–39. https://doi.org/10.1360/972010-1322.
Gao, P., Wang, P., Chen, S., Bi, W., Lu, S., He, J., et al., 2020. Effect of ambient nitrogen on the growth of phytoplankton in the Bohai Sea: Kinetics and parameters. J. Geophys. Res. Biogeo. 125, e2020JG005643 https://doi.org/10.1029/2020JG005643.
Goswami, L., Kumar, R.V., Manikandan, N.A., Pakshirajan, K., Pugazhenthi, G., 2017. Simultaneous polycyclic aromatic hydrocarbon degradation and lipid accumulation by Rhodococcus opacus for potential biodiesel production. J. Water Process. Eng. 17, 1–10. https://doi.org/10.1016/j.jwpe.2017.02.009.
Goswami, L., Kumar, R.V., Manikandan, N.A., Pakshirajan, K., Pugazhenthi, G., 2019. Anthracene biodegradation by oleaginous Rhodococcus opacus for biodiesel production and its characterization. Polycycl. Aromat. Comp. 39 (3), 207–219. https://doi.org/10.1080/10406638.2017.1302971.
Goswami, L., Manikandan, N.A., Dolman, B., Pakshirajan, K., Pugazhenthi, G., 2018. Biological treatment of wastewater containing a mixture of polycyclic aromatic hydrocarbons using the oleaginous bacterium Rhodococcus opacus. J. Clean. Prod. 196, 1282–1291. https://doi.org/10.1016/j.jclepro.2018.06.070.
Hao, X., Li, J., Yao, Z., 2016. Changes in PAHs levels in edible oils during deep-frying process. Food Contr 66, 233e240. https://doi.org/10.1016/j.foodcont.2016.02.012.
Ho, Y.S., Mckay, G., 1999. Pseudo-second order model for sorption processes. Process Biochem 34 (5), 451–465. https://doi.org/10.1016/s0032-9592(98)00112-5.
Hu, L., Guo, Z., Shi, X., Qin, Y., Lei, K., Zhang, G., 2011. Temporal trends of aliphatic and polyaromatic hydrocarbons in the Bohai Sea, China: evidence from the sedimentary record. Org. Geochem. 42 (10), 1181–1193. https://doi.org/10.1016/j.orggeochem.2011.08.009.
Hu, N., Shi, X., Liu, J., Huang, P., Liu, Y., Liu, Y., 2010. Concentrations and possible sources of PAHs in sediments from Bohai Bay and adjacent shelf. Environ. Earth Sci. 60 (8), 1771–1782. https://doi.org/10.1007/s12665-009-0313-0.
IARC., 2007. IARC, International Agency for Research on Cancer.
Jones, K.C., Voogt, P.D., 1999. Persistent organic pollutants (POPs): state of the science. Environ. Pollut. 100 (1-3), 209–221. https://doi.org/10.1016/s0269-7491(99)00098-6.
Lara-Martin, P.A., Chiaia-Hernandez, A.C., Biel-Maeso, M., Baena-Nogueras, R.M., Hollender, J., 2020. Tracing urban wastewater contaminants into the Atlantic Ocean by nontarget screening. Environ. Sci. Technol. 54, 3996–4005. https://doi.org/10.1021/acs.est.9b06114.
Li, W., Zu, B., Li, Z.L., Wang, J., 2018. Research progress of adsorption and desorption of phosphate in sediment. Environ. Prot. Sci. 44 (4), 49–53. https://doi.org/10.3969/j.issn.0517-6611.2019.01.002.
Malwade, K., Lataya, D., Mhaisalkar, V., Kurwadkar, S., Ramirez, D., 2016. Adsorption of hexavalent chromium onto activated carbon derived from Leucaena leucocephala waste sawdust: kinetics, equilibrium and thermodynamics. Environ. Sci. Technol. 13, 2107–2116. https://doi.org/10.1007/s13762-016-1042-z.
Neroda, A.S., Goncharova, A.A., Mishukov, V.F., 2020. PAHs in the atmospheric aerosols and seawater in the North-West Pacific ocean and sea of Japan. Atmos. Environ. 222, 117117 https://doi.org/10.1016/j.atmosenv.2019.117117.
Nzengung, V.A., Nkedi-Kizza, P., Jessup, R.E., Voudrias, E.A., 1997. Organic cosolvent effects on sorption kinetics of hydrophobic organic chemicals by organoclays. Environ. Sci. Technol. 31, 1470–1475. https://doi.org/10.1021/es960720z.
Oh, S.H., Qi, W., Song, D.I., Shin, W.S., 2011. Sorption and desorption kinetics of naphthalene and phenanthrene on black carbon in sediment. J. Soil Groundw. Environ. 16 (6), 79–94. https://doi.org/10.7857/jsge.2011.16.6.079.
Oh, S.H., Wang, Q., Shin, W.S., Song, D.I., 2013. Sorption and desorption kinetics of pahs in coastal sediment. Korean J. Chem. Eng. 30 (1), 145–153. https://doi.org/10.1007/s11814-012-0101-5.
Sahu, M.K., Patel, R.K., Kurwadkar, S., 2022. Mechanistic insight into the adsorption of mercury (II) on the surface of red mud supported nanoscale zero-valent iron composite. J. Contam. Hydrol. 246, 103959 https://doi.org/10.1016/j.jconhyd.2022.103959.
Sakellari, A., Karavoltsos, S., Moutafis, I., Bakeas, E., 2021. Occurrence and distribution of polycyclic aromatic hydrocarbons in the marine surface microlayer of an industrialized coastal area in the eastern mediterranean. Water 13, 3174. https://doi.org/10.3390/w13223174.
Shi, W., Xu, M., Liu, Q., Xie, S., 2022. Polycyclic aromatic hydrocarbons in seawater, surface sediment, and marine organisms of Haizhou Bay in Yellow Sea, china: distribution, source apportionment, and health risk assessment. Mar. Pollut. Bull. 174, 1–10. https://doi.org/10.1016/j.marpolbul.2021.113280.
Shi, B.F., Zuo, W.Y., Tong, H.J., 2015. Adsorption of polycyclic aromatic hydrocarbons from aqueous solutions using modified bentonite. Chin. J. Environ. Eng. 9 (4), 1680–1686 https://doi.org/CNKI:SUN:HJJZ.0.2015-04-026.
Sun, Y., Xie, Z., Wu, K., Lan, J., Li, T., Yuan, D., 2021. Speciation, distribution and migration pathways of polycyclic aromatic hydrocarbons in a typical underground river system in Southwest China. J. Hydrol. 596, 125690 https://doi.org/10.1016/j.jhydrol.2020.125690.
Tao, Y.Q., Yu, J., Xue, B., Yao, S.C., Wang, S.M., 2017. Precipitation and temperature drive seasonal variation in bioaccumulation of polycyclic aromatic hydrocarbons in the planktonic food webs of a subtropical shallow eutrophic lake in China. Sci. Total Environ. 583, 447–457. https://doi.org/10.1016/j.scitotenv.2017.01.100.
Tuzen, M., Sari, A., Mendil, D., Soylak, M., 2009. Biosorptive removal of mercury (II) from aqueous solution using lichen (Xanthoparmelia conspersa) biomass: kinetic and equilibrium studies. J. Hazard. Mater. 169, 263–270. https://doi.org/10.1016/j.jhazmat.2009.03.096.
USEPA., 1992. Guidelines for Exposure Assessment. Risk Assessment Forum. U.S. Environmental Protection Agency, Washington, DC.
Vento, S.D., Dachs, J., 2002. Prediction of uptake dynamics of persistent organic pollutants by bacteria and phytoplankton. Environ. Toxicol. Chem. 21 (10), 2099–2107. https://doi.org/10.1002/etc.5620211013.
Walter, J.R., Waber, J., Huang, W., 1996. A distributed reactivity model for sorption by soils and sediments. 4. intraparticle heterogeneity and phase-distribution relationships under nonequilibrium conditions. Environ. Sci. Technol. 30 (3), 881–888. https://doi.org/10.1021/es950329y.
Wang, A., Guo, X., Shi, J., Luo, C., Gao, H., 2019. A simulation of the seasonal variation of decabromodiphenyl ether in a bay adjacent to the Yellow Sea. Sci. Total Environ. 664, 522–535. https://doi.org/10.1016/j.scitotenv.2019.01.385.
Wang, L., Niu, J., Yang, Z., Shen, Z., Wang, J., 2008. Effects of carbonate and organic matter on sorption and desorption behavior of polycyclic aromatic hydrocarbons in the sediments from Yangtze River. J. Hazard. Mater. 154 (1-3), 811–817. https://doi.org/10.1016/j.jhazmat.2007.10.096.
Wang, W., Simonich, S., Giri, B., Chang, Y., Zhang, Y., Jia, Y., et al., 2011. Atmospheric concentrations and air-soil gas exchange of polycyclic aromatic hydrocarbons (PAHs) in remote, rural village and urban areas of Beijing-Tianjin region, North China. Sci. Total Environ. 409 (15), 2942–2950. https://doi.org/10.1016/j.scitotenv.2011.04.021.
Wang, C., Thakuri, B., Roy, A.K., Mondal, N., Chakraborty, A., 2022. Phase partitioning effects on seasonal compositions and distributions of terrigenous polycyclic aromatic hydrocarbons along the South China Sea and East China Sea. Sci. Total Environ. 828, 154430 https://doi.org/10.1016/j.scitotenv.2022.154430.
Wang, N., Wang, Y.P., Duan, X., Wang, J., Xie, Y., Dong, C., et al., 2020. Controlling factors for the distribution of typical organic pollutants in the surface sediment of a macrotidal bay. Environ. Sci. Pollut. R. 27, 28276–28287. https://doi.org/10.1007/s11356-020-09199-w.
Werner, D., Karapanagioti, H.K., Sabatini, D.A., 2012. Assessing the effect of grain-scale sorption rate limitations on the fate of hydrophobic organic groundwater pollutants. J. Contam. Hydrol. 129-130, 70–79. https://doi.org/10.1016/j.jconhyd.2011.10.002.
Wu, F.C., Tseng, R.L., Huang, S.C., Juang, R.S., 2009. Characteristics of pseudo-second-order kinetic model for liquid-phase adsorption: a mini-review. Chem. Eng. J. 151 (1-3), 1–9. https://doi.org/10.1016/j.cej.2009.02.024.
Xing, B., Pignatello, J.J., 1997. Dual-mode sorption of low-polarity compounds in glassy poly (vinyl chloride) and soil organic matter. Environ. Sci. Technol. 31 (3), 792–799. https://doi.org/10.1021/es960481f.
Xu, X.W., Huang, S.L., 2011. Adsorption-desorption behaviors of phenanthrene on sediments from the Haihe River. Acta Sci. Circumstantiae 31 (1), 114–122. https://doi.org/10.7666/d.y1813877.
Xu, B., Liu, F., Alfaro, D., Jin, Z., Liu, Y., Liu, Y., et al., 2022. Polycyclic aromatic hydrocarbons in fine road dust from a coal-utilization city: spatial distribution, source diagnosis and risk assessment. Chemosphere 286, 131555. https://doi.org/10.1016/j.chemosphere.2021.131555.
Yang, G.P., Zheng, X., 2010. Studies on the sorption behaviors of phenanthrene on marine sediments. Environ. Toxicol. Chem. 29 (10), 2169–2176. https://doi.org/10.1002/etc.270.
Zafarani, G.G., Karbalaei, S., Golshani, R., Pustokhina, I., Walker, T.R., 2022. Baseline occurrence, distribution and sources of PAHs, TPH, and OCPs in surface sediments in Gorgan Bay, Iran. Mar. Pollut. Bull. 175, 113346 https://doi.org/10.1016/j.marpolbul.2022.113346.
Zhang, D., Duan, D., Huang, Y., Xiong, Y., Yang, Y., Ran, Y., 2016. Role of structure, accessibility and microporosity on sorption of phenanthrene and nonylphenol by sediments and their fractions. Environ. Pollut. 219 (Dec), 456–465. https://doi.org/10.1016/j.envpol.2016.05.052.
Zhang, Y.D., Tian, S.Y., Liu, X.B., Li, G.F., Zhu, W.J., Jia, R., 2013. Distribution, source and ecological risk assessment of polycyclic aromatic hydrocarbons in surface water from the northwest Bohai Sea. China Oceanol. Limnol. Sin. 44 (1), 255–261. https://doi.org/10.11693/hyhz201301038038.

Zheng, X., 2010. Studies on the sorption behaviors of phenanthrene and methylene blue on marine sediments. master's thesis, the Ocean University of China, Shandong, Qingdao. https://doi.org/10.7666/d.y1830235.
Zheng, Z.Z., Li, H.Y., 2017. Pollution status and research progress of polycyclic aromatic hydrocarbons in water environment. Adm. Tech. Environ. Monit. 29 (5), 1–6. https://doi.org/10.19501/j.cnki.1006-2009.2017.05.001.
Zhu, K., Zhan, H.Y., Wang, E.P., Xie, C.J., 2006. Sorption of phenanthrene and naphthalene in natural and HDTMA-modified loess soils. J. Agro Environ. Sci. 25 (4), 958–963. https://doi.org/10.3321/j.issn:1672-2043.2006.04.028.